

Optics Study for ALMA Receivers

James Lamb¹

Abstract— The design of the receiver optics plays a crucial part in the ultimate sensitivity of the ALMA array. We present some general design concepts to guide the development of the optical layout of the final receivers. Relevant properties of materials used in the optical path are examined, and various types of optical elements are discussed. General principles of high efficiency optical train designs are presented. In general, simple systems are advocated, with minimal truncation losses. The areas which have the greatest uncertainty are the windows and infrared filters where the trade-offs between the RF losses, infrared blocking, pressure resistance and gas permeability have to be carefully considered. A sample design for Band 3 is given.

I. INTRODUCTION

The number of receivers, frequency coverage, and sensitivity required to take full advantage of the excellent atmospheric transparency on the ALMA site make the receiver design for the ALMA instrument a critical and challenging task. It is clear that achieving the highest sensitivity is of paramount importance, so this note presents a detailed study of relevant optical design factors.

The sensitivity of an interferometer array (*i.e.*, the minimum signal which can be detected in a given integration time) depends on the number and size of antennas; the aperture efficiency; the system noise temperature; the relative pathlength stability between antennas; the processed bandwidth; and the correlator efficiency [1]. Point-source and extended-source sensitivities are differentiated by the antenna number and size only so the distinction is unimportant in the context of this note. The most important considerations for the optics are the system noise temperature and the aperture efficiency. These parameters depend on the plane of reference, but they can be combined to give the system noise power relative to the output power due to a point source with a given flux. It is this measure that is implicitly calculated in the remainder of the document. Phase stability can be affected by optics through vibration but careful mechanical design can reduce this to negligible levels. Bandwidth is limited by the intermediate frequency system rather than the optics.

By examining a variety of options and carefully evaluating trade-offs and constraints we can hope to arrive at a design that will be flexible, allow the highest sensitivity to be

achieved and define a system that can be easily maintained over its lifetime. As a benchmark we note that to achieve a 1 % enhancement in sensitivity by increasing the collecting area of the array would cost an estimated \$US 2–3M. Although this document does not deal directly with cost, reliability, or maintenance issues it gives sufficient details of optical performance evaluation for the trade-offs to be examined once those other issues are addressed.

Since the optics is an area where sensitivity may be easily compromised, this memo discusses performance of low-loss optics in detail. Relevant concerns are: dissipative and scattering losses; spillover losses; receiver and telescope aberrations; window sizes; materials; infrared filters; feed elements; frequency dependence; and geometrical constraints.

We start with a general discussion of the effects of optical losses on system performance. This is followed by a survey of the properties of materials available for millimeter and sub-millimeter optical components. Pertinent characteristics of various optical elements and their influence on performance are covered. Finally, we look at general design principles for high performance optical systems illustrated by a design example. This uses concepts of paraxial beams including higher order effects required to describe the non-Gaussian nature of real feeds. All the parameters affecting sensitivity by a fraction of a percent or more are discussed quantitatively.

II. EFFECT OF LOSSES ON SENSITIVITY

All optical components will have some associated loss which must be figured into the sensitivity budget. These losses will contribute to the system noise temperature by adding noise and by multiplying up the noise of following components. For a component with a loss L at a physical temperature T_{phys} placed in front of a receiver with noise temperature T_{Rx} the fractional increment in system noise is

$$\frac{\Delta T}{T_{Rx}} = (L-1) \left(\frac{T_{phys}}{T_{Rx}} + 1 \right) \quad (1)$$

This shows that for a given loss the relative degradation is worse for a low-noise receiver. For $T_{Rx} \ll T_{phys}$ the degradation factor is much worse than the loss. For example, for a 1 % loss ($L = 1.01$) at $T_{phys} = 300$ K in front of a 30 K receiver we find $\Delta T/T_{Rx} = 11$ %. For a 300 K receiver the change is only 2 %. Clearly, low-noise systems are

*This note is based on a presentation given at a meeting of the Joint Receiver Development Group in Grenoble, December 1999.

25 March, 2001

¹Owens Valley Radio Observatory, California Institute of Technology, Big Pine, CA 93513, USA

* Loss is defined as the incident power over transmitted (or reflected) power.

particularly sensitive to losses at ambient temperature. Cooling optical components is therefore very beneficial since it generally reduces the both factors in Eq. (1). We can expect $T_{Rx} \ll 300$ K for millimeter systems and $T_{Rx} \approx 300$ K for sub-millimeter receivers, so that cooling the optics will have most benefit for the low frequencies; nevertheless, it will also appreciably improve the higher frequency bands.

For losses due to reflections, truncation, and scattering the termination temperature is not the component temperature, and T_{phys} in (1) must be replaced by the temperature of the surroundings that the radiation is scattered to. For a truncating aperture there will be some power intercepted by the aperture. Often this power is reflected back into the cryogenic stages so has a low effective noise temperature. In addition, there is an equal amount of power diffracted out of the main beam. This power may be terminated partially on the sky and partially in the local surroundings. At a mirror the power that spills past the edge will generally be terminated at the local ambient (room temperature or cryogenic temperature). Again, there is an equal amount of diffraction loss.

Surface errors scatter power from the optical beam. Large-scale errors result in scattering of power at angles near to the main beam. This power will propagate through an optical system having reasonably large clearances and be terminated on the sky. Small-scale errors will scatter to the local surroundings. Since it is easier to maintain surface accuracy on small scales it is reasonable to expect that less than half the power will be terminated at ambient, so this loss is not as detrimental as is often assumed.

With careful design all the losses will be of a similar magnitude. As will be clear in the following sections, great care has to be taken with truncation losses. Using simple Gaussian beams may give misleading results, and more realistic beams have to be assumed.

III. OPTICAL MATERIALS

Optical materials for millimeter wavelengths include: metals for grids and reflectors; dielectrics for lenses, windows and IR filters; and ferrites for isolators. Isolators are not widely used in low-loss optical systems so we will not discuss them further. The other materials will contribute small but significant losses that need to be evaluated, and the relative merits are compared in the following sections. A compendium of materials that may be used in millimeter wave optics may be found in [2].

A. Metals

Metallic surfaces are used for plane and focusing mirrors and wire grid polarizers. At a frequency ν the reflection loss L at a metallic surface with conductivity σ is found from

$$1 - L^{-1} = 4 \sqrt{\frac{\pi \epsilon_0 \nu}{\sigma}} \quad (2)$$

where ϵ_0 is the dielectric constant of free-space. Surface roughness typically reduces the effective conductivity in proportion to the increase in surface area on the microscopic

scale [3]. At non-normal incidence the losses increase and are different for the TE and TM fields [4], but these effects are generally small enough to ignore for the systems and wavelengths considered here.

Conductivities of metals depend on the type and structure of the bulk material and its surface finish. DC conductivity may be used as a guide for estimating RF losses, but the effective loss at millimeter and sub-millimeter wavelengths may be significantly higher. With careful surface preparation the discrepancy between DC and effective GHz or THz conductivity values can be less than a factor of two. There are few direct measurements of Ohmic losses at millimeter and sub-millimeter wavelengths. In the sub-millimeter range conductivities of $1.6\text{--}3 \times 10^7$ S m⁻¹ have been measured between room temperature and 200 K for aluminum and its alloys, and $1.8\text{--}4.6 \times 10^7$ S m⁻¹ for bulk copper [5], [6].

The most accurate measurements that we know of are those at 584 GHz by Gatesman *et al.* [7]. They found that the reflection losses for copper, silver, gold and aluminum are 0.3 %, 0.4 %, 0.6 %, and 0.5 % respectively for carefully prepared samples. For commercially available front surfaced mirrors the loss increases to 0.8 % for ‘enhanced aluminum’ and 1.5 % for ‘protected aluminum’. Measurements by Bock *et al.* [8] confirm that reflectivities consistent with bulk DC conductivities are achievable.

Some components will be cryogenically cooled but most RF loss measurements are made at room temperature. It is less important to know low temperature values precisely since the thermal emission is greatly reduced, improving sensitivity even in the absence of resistivity reduction (see Sec. II). Aluminum alloys and copper do in fact show increases in DC conductivities at 4 K by factors from 2 to 100, with the lower resistivity materials improving more [9]. At millimeter and sub-millimeter wavelengths the conductivity relative to DC can be slightly increased at ambient due to Drude relaxation, or decreased at low temperatures due to anomalous skin depth, but these effects are generally negligible.

For the ALMA receivers careful attention should be paid to the preparation of the reflecting surfaces, particularly those at ambient-temperature. Copper plated surfaces are very low-loss, but the long-term behavior would need to be verified.

B. Dielectrics

Losses in dielectrics depend on many factors. Significant variations in reported values are seen because of different material suppliers, sample preparations, and methods of measurement. Many materials have absorption features near or in the millimeter/sub-millimeter so that losses and dielectric constants can change rapidly with frequency. There are few results of measurements on very low-loss materials at cryogenic temperatures. Small increases in loss with decreasing temperatures have been seen in some materials and orders of magnitude decrease have been observed in others (see the tables in [2], for example).

For a low-loss dielectric with a refractive index n , a loss tangent $\tan \delta$ (ratio of real to imaginary parts of the dielectric constant) and thickness t the loss at a wavelength λ is

$$1 - L^{-1} = t \frac{2\pi\nu}{c} \tan \delta = \frac{t}{\lambda_d} \tan \delta \quad (3)$$

In comparing materials we must remember that the required thickness will depend on the material properties and the frequency. For vacuum windows the thickness will depend on the mechanical strength and permeability of the dielectric; for IR filter applications it depends on the optical depth in the IR; and for lenses it depends on focal length and is proportional to $(n-1)^{-1}$. At higher frequencies the signal beams are smaller and the component dimensions commensurately reduced. Depending on these factors, typical losses are in the range of a fraction of a percent to a few percent.

Some materials (notably foams) also exhibit scattering losses. This attenuates the signal and may also scatter ambient temperature radiation into the receiver. Measurements reported in [10] on a foam window showed scattering of about 1 % of the beam at 260 GHz.

The most common materials are PTFE* (Teflon), HDPE, and TPX. Properly prepared PTFE has the lowest loss at frequencies below 200–300 GHz. It becomes lossier at higher frequencies, but the reported frequency range where the loss increases varies between different publications, probably because of differences in the manufacturing process. Physically, it is denser than HDPE, but is more pliable at cryogenic temperatures and thus less likely to fracture. At higher frequencies, HDPE has significantly lower loss. Quartz is also used, but it is more expensive to fabricate and the high dielectric constant makes it more difficult to match to free space.

At cryogenic temperatures the dielectric constant changes. In cases where no measured values are available the Lorentz-Lorenz relationship [4], which relates dielectric constant and density, will often yield a sufficiently accurate value for the dielectric constant [2]. Density change is found from published thermal contraction values or simply by cooling a sample in liquid nitrogen and measuring the dimensional change directly.

C. Examples

Comparison of different materials used for lenses, windows, mirrors, *etc.*, may be made by quantifying their effects on the sensitivity of the entire system. As a basis for the comparison we take the parameters shown in Table I.

TABLE I
SOME OF THE PARAMETERS USED IN THE CALCULATIONS OF SENSITIVITY LOSS DUE TO VARIOUS OPTICAL CONFIGURATIONS.

Parameter	Value
Atmospheric precipitable water vapor	1 mm
Air masses at observing elevation	1
Receiver noise temperature	$2h\nu/k$, $4h\nu/k$, $10h\nu/k$
Antenna spillover efficiency	95 %, 98 %

* PTFE has a phase transition at 18 °C which is a concern for phase stability of cables, but it does not appear to have been a problem for lenses.

Three cases representing some typical components are considered as follows:

Case I: A two mirror system with $\sigma = 2 \times 10^7 \text{ S m}^{-1}$ at room temperature. Two mirrors are considered since a second mirror is often required to redirect the beam in the appropriate direction, even though it may not be needed for imaging.

Case II: An HDPE window at room temperature with a thickness of λ/n . The thickness can be scaled with wavelength because the beam diameter will shrink and the thickness can be reduced accordingly.

Case III: An HDPE lens at 4 K with a thickness of $5\lambda/(n-1) + 1 \text{ mm}$, which accounts for a focal length proportional to wavelength plus a 1 mm thick flange.

To simplify calculation, component dimensions are assumed to scale continuously with wavelength, but in practice they will be fixed within a given band. The total reduction in sensitivity includes both the added thermal noise and the multiplication of the following receiver noise.

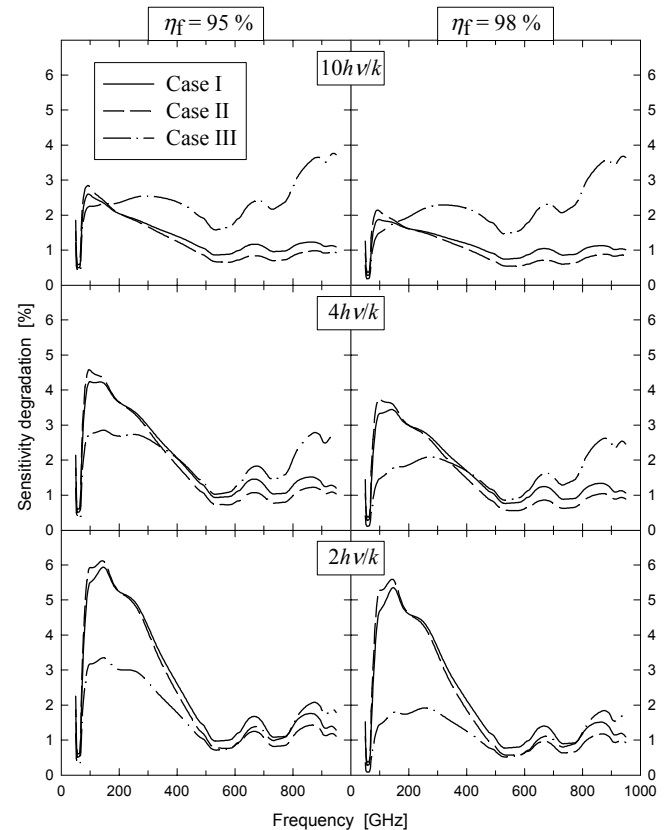


Fig. 1. Reduction of system sensitivity for different optical components and various values of the parameters

Fig. 1 shows the relative degradation of receiver noise for these example cases. No scattering or spillover losses in the optics are included but those will be very important in a real implementation (see Sec. VI). In general the greatest degrada-

tion is at the lower end of the frequency range, most significantly in the 2-mm wavelength window. At the higher frequencies the added noise is lower relative to the receiver noise because: the receiver noise increases (the quantum limit is proportional to frequency); the thermal noise in the Planck spectrum decreases; and atmospheric transparency becomes worse. At first sight the cryogenic lens appears to be more favorable than the dual reflectors at ambient temperature. However the reflectors would allow a smaller window in the cryostat and therefore thinner vacuum windows and IR filters. For reference the noise contributed by a reflector is equivalent to only one or two millimeters thickness of dielectric at ambient temperature.

IV. OPTICAL COMPONENTS

Some of the typical components used in the optics are discussed in the following sections.

A. Feed Horns

While several types of feed have been used in the millimeter wavelength regime none has exceeded the performance of the corrugated horn—it is in effect the “gold standard” for waveguide feeds. It maintains high efficiency, low cross-polarization, a spherical wavefront, low loss and high return loss over large bandwidths (~40 %) [11]. At low frequencies (<370 GHz) the fabrication is relatively straightforward, but horns have been successfully manufactured and tested up to 2.4 THz [12]. Diagonal horns [13] are relatively simple to make, but have poor phase and cross-polarization characteristics. Potter horns [14] have better patterns, but are more limited in bandwidth than corrugated feeds.

Often the simpler types of horn are used as feeds for local oscillator (LO) injection where beam quality is less crucial. However, corrugated horns should also be considered for LO injection in the ALMA receivers. An efficient production method will be needed for the 70–140 horns required for each of the ALMA receiver bands, and it should not be a significantly greater effort to make them for LO injection as well as for signal coupling. The main benefit is that improved match should lead to better stability and less LO leakage between bands, but the slight improvement in coupling at band edges may also be important.

Very low VSWR transitions for corrugated feeds have been designed by using slots in the throat section of the horn that become narrower towards the horn apex [15]. However, as shown in Fig. 2, a design with constant-width slots can achieve a very low return loss over a 40 % bandwidth [16], which is larger than any of the bands proposed for ALMA [17].

It is often assumed that the aperture field of the horn is given by a truncated zeroth order Bessel function amplitude distribution with a spherical wavefront. Computations for a real feed using a mode-matching program [18] show that this is a good approximation over the band of the horn (Fig. 3). Calculations of the coupling to the telescope with the simplified and the more accurate fields show differences of less than 1 %.

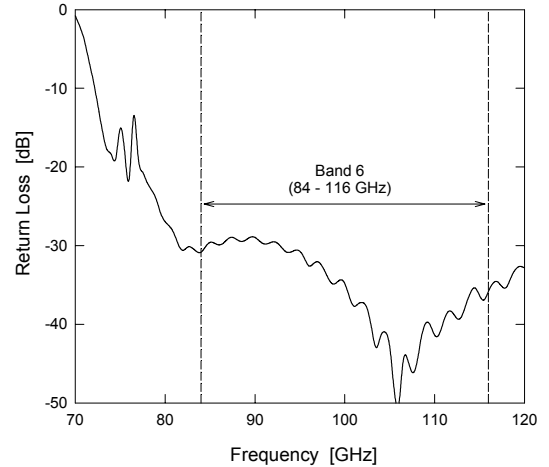


Fig. 2. Reflection loss calculated for corrugated horn for Band 3 of ALMA Prototype Antenna Evaluation Receiver.

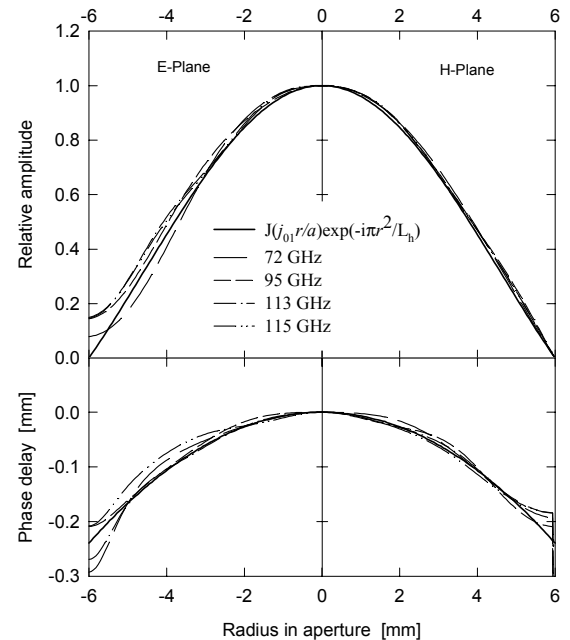


Fig. 3. Horn aperture field computed for a corrugated horn using mode-matching software. Comparison is made with the usual simplifying assumption of a spherical wavefront and Bessel function amplitude.

B. Planar Feeds

Quasi-optical or planar feeds may be used at the higher frequencies. The most successful designs have based on twin-slot antennas with hyperhemispherical lenses [19]. In the following sections it is assumed that a corrugated horn is used, but this could be replaced by a planar feed with optics to generate a similar beam. Efficiencies would then have to be appropriately re-evaluated.

C. Lenses

Lenses are often used in millimeter optical systems and are relatively easy to manufacture on a lathe. The tolerances are

less stringent than for mirrors by a factor of $(n-1)$, which is typically ~ 0.5 , but this is offset by the greater difficulty in achieving this tolerance in the softer surface of a dielectric. Furthermore, lenses have two surfaces to be machined, each with its contribution to the surface accuracy.

Lenses do not change the direction of propagation of the beam, which can be advantageous in some cases and inconvenient in others. The resulting axial symmetry makes it relatively easy to align the lens with the optical axis.

Reflection at a dielectric surface is significant and usually some type of anti-reflection treatment is applied to the lens surface. Typically this is in the form of concentric grooves machined into the lens surfaces. These, however, generate astigmatism and cross-polarization with a corresponding loss of 0.3–2 % for the two surfaces [20]. With the wide availability of numerically controlled machines it is now practical to make an isotropic matching layer by drilling a large number of holes into the lens surface [21].

Having two surfaces also opens the possibility of shaping the illumination pattern to improve the antenna aperture efficiency [22], [23], [24].

D. Focusing Mirrors

Mirrors are often favored over lenses because of their lower loss, as well as the much lower VSWR. However reflectors are almost invariably used at non-normal incidence which results in non-axisymmetric optics and a deviation of the beam direction. These factors can make it harder to align mirrors, unless the mirror (or at least the center) is polished for laser alignment—lens materials are generally too opaque to allow this.

The asymmetry is also responsible for some losses. For a single mirror with a focal length f the loss from a fundamental Gaussian mode into higher order co-polar modes with the same plane polarization is approximately [25]

$$L = \frac{1}{8} \frac{w}{f} \tan^2(i) \quad (4)$$

where w is the radius of the Gaussian beam at the mirror and i is the incidence angle. Loss into cross-polar components is twice this. Although these losses are not necessarily a true loss of signal (*e.g.*, coupling to an extended source), they do correspond to loss of point source sensitivity as they translate to increased sidelobes. The cross-polarization will directly affect polarization mapping accuracy.

Obviously small incidence angles and large f -ratio mirrors are indicated. In the design of a focusing mirror it is often necessary to find a compromise between the geometrical problems incurred by requiring small angles of incidence, with the increased loss and cross-polarization associated with larger incidence angles.

Sometimes these effects may be ameliorated or eliminated by combining two or more focusing reflectors. There have been several treatments of combinations of optical elements with cross-polar components that cancel. The most comprehensive is the paper by Dragone [26], which gives the geometrical conditions for trains of conic section reflectors. The

analysis uses geometric optics (GO) so it is not fully applicable to quasi-optical systems (though it is the correct limiting case). In the GO analysis the distortion produced by one mirror propagates to the second mirror unchanged except for a scaling factor. The second mirror then just has to have the same distortion to return the beam to its original distribution (Fig. 4a). If the beam passes through a focus the distortion and cross-polarization patterns are inverted, requiring the second mirror to be inverted (Fig. 4b).

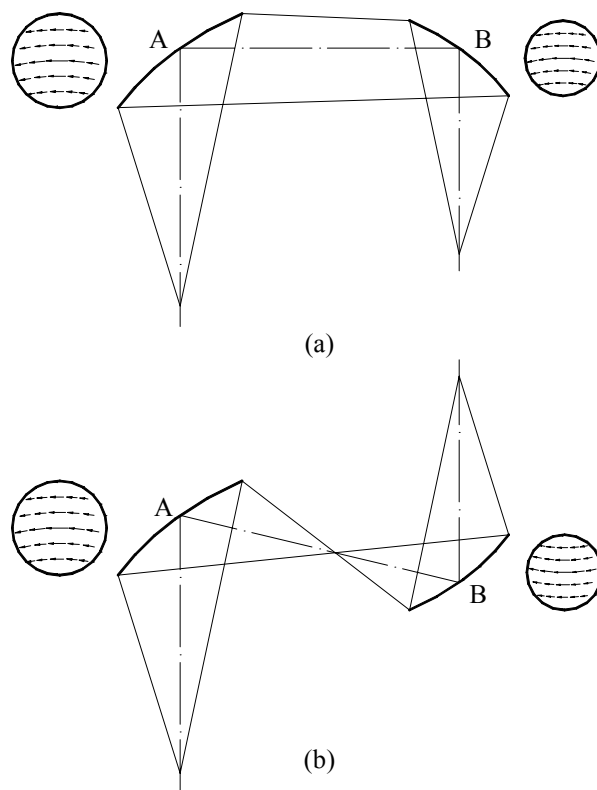


Fig. 4. Two possible geometrical arrangements of mirrors that can give cancellation of distortion and cross-polarization. The mirrors must keep the beam axis in the same plane and must have the same orientation if there is no intermediate focus (a), or one must be inverted if there is a focus between the mirrors (b).

In the quasi-optical analysis, if a fundamental Gaussian mode is incident on Mirror A the distortion and cross-polarization can be represented by antisymmetric higher order modes [25]. As they propagate from mirror A to Mirror B, these higher order modes will slip in phase relative to the fundamental [27]. A small phase slippage corresponds to Fig. 4a, while a phase slippage of $\sim \pi$ corresponds to Fig. 4b. (It is easily seen that resultant field obtained by adding an antisymmetric mode with a phase of π to a symmetric mode is an inverted image of the field obtained from a symmetric mode and an in-phase antisymmetric mode.) If the phase slippage is not close to zero or π the resultant field will also have a phase error at Mirror B which will not be compensated by it. Chu [28] discusses this in detail for a dual-reflector antenna and quantifies the loss in terms of the phase slippage parameter.

One important deduction from this is that cross-polar in the receiver optics will generally not cancel the cross-polar due to the feed offset very well. This is because the optics are near the secondary mirror, and the phase slippage from the secondary focus to the secondary mirror is $\sim\pi/2$ so that the high-order cross-polar modes add in phase quadrature. At the higher frequencies the optics can be further from the focus and the cancellation may be somewhat better.

Another effect not present in GO is the displacement of the phase centers of the input and output beam as a function of frequency. This appears as a comatic aberration, and Withington *et al.* [29] derive a closed form for the associated loss:

$$1 - L^{-1} = \left(\frac{\pi w_m^3 \tan(i)}{\lambda} \left(\left(\frac{1}{R_{mi}^2} - \frac{1}{R_i^2} \right) + \left(\frac{1}{R_{mo}^2} - \frac{1}{R_{oi}^2} \right) \right) \right)^2 \quad (5)$$

R_i and R_o are the radii of curvature of the input and output beams, w is the beam radius at the mirror, and the subscript m denotes the values at mid-band.

E. Infrared Filters

Several types of infrared filters have been used for millimeter and submillimeter receivers. Various materials which have absorption bands in the infrared but are transparent at longer wavelengths have been successfully employed [30], [31]. Some of these are solid materials, such as PTFE, Fluorogold and Fluorosint (both based on PTFE). Because of the appreciable dielectric constant, the interface reflections need to be taken into account. Rectangular or triangular matching grooves [32] can be machined into the surface to reduce the reflections. Triangular grooves give a larger matching bandwidth, but the depth is large compared to the pitch making fabrication harder. In large filters, significant temperature gradients can exist from the center of the filter to the periphery where they contact the cryogenic stations. This reduces their effectiveness [31] and the thickness may have to be increased to compensate, to the detriment of the RF loss.

Fused quartz can also be utilised and is generally matched with PTFE layers. However, due to the relatively high dielectric constant of quartz, the VSWR is not acceptable for ALMA requirements [33]. Furthermore, effective attachment of PTFE is difficult in the face of cryogenic temperature cycling. Multilayer antireflection layers will increase the usable bandwidth, but this is a relatively complicated solution with more risk of delamination at low temperatures. Quartz has a higher thermal conductivity than PTFE [34], but significant temperature gradients may still exist in large filters since thinner material will probably be required (for RF losses).

Materials with lower dielectric constants such as foamed polystyrene or PTFE are also useful. Because of the extremely low thermal conductivity there are large temperature gradients from the front to the back of the foam and it acts like multi-layer insulation, re-radiating back to the source. This has the benefit that the loading on the cryocooler is reduced relative to a solid absorbing filter. Measurements of the infrared and submillimeter transmission of an expanded PTFE material (Zitex [35]) have been made by Benford *et al.*

[36] and the IR blocking properties investigated by Clarke and D'Addario [37]. This material is a very good filter candidate because of its high IR opacity and high (sub-)millimeter transparency.

Other possibilities for infrared blocking include interference filters and diffraction gratings. Interference filters could be made by evaporating thin films on to a substrate to reflect IR but transmit millimeter and sub-millimeter radiation. Silicon would be an ideal substrate apart from its high dielectric constant. If a nitride etch-stop layer is formed on the top to suspend the thin films, holes could be etched into the back of the silicon to reduce the effective dielectric constant (provided the hole spacing is less than half-a wavelength at the highest sub-millimeter frequency) [38]. Preliminary calculations reveal that the filling factor for the holes has to be very high, and further investigation is needed to see if this is practical. It does appear that a significant amount of rejection of IR could be achieved along with low loss for the signal beam. An attraction of this type of filter is that it does not cause any extra loading on any of the cryogenic stages.

Reflective diffraction gratings (blazed echelles) also offer the potential of reduced loading on all stages by diffractively separating the IR and RF [39]. Unlike transmitting filters, reflective ones cannot cover the entire aperture and special baffles are needed to prevent IR from going round the edges of the grating. Some of the difficulties of the geometry are illustrated in Fig. 5.

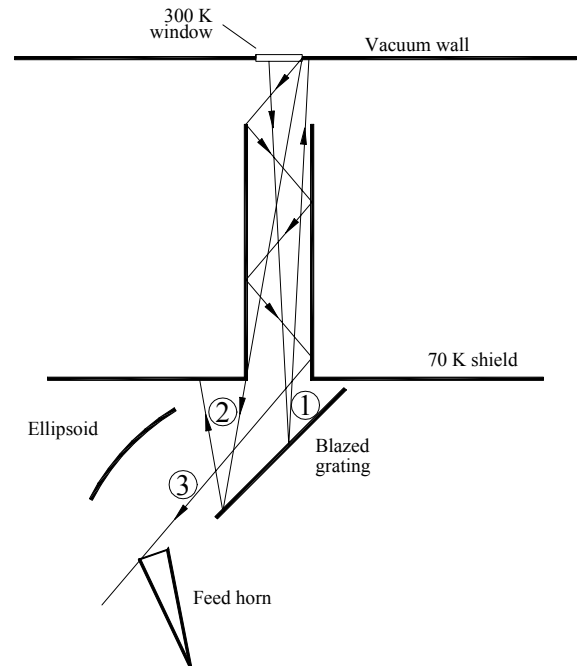


Fig. 5. A blazed grating can be used to diffractively separate IR and mm or sub-mm waves. In this diagram the grating is designed to send IR coming in parallel to the optical axis back along the same path. Rays incident at other angles may be reflected to the interior of the vacuum vessel, (1), or the radiation shield, (2). Highly oblique rays can be reflected multiple times and not be intercepted by the grating (3). By making the interior of the tube absorptive this is avoided, though the thermal load is transferred to the shield.

F. Vacuum Windows

Several vacuum window designs are in current use, though none are perhaps ideal. Optical requirements for low reflection, scattering, and loss generally conflict with the requirements for impermeability to gasses (particularly water vapor), and resistance to atmospheric pressure.

Thin membranes, such as Mylar (PETP) are strong but have to be thin to avoid losses and reflections. Relatively large windows have been made by backing the membrane with a strong foam to resist atmospheric pressure [10]. A side effect is that the foam also acts as an IR block [31].

However, Mylar is somewhat permeable to water and helium and lossy at millimeter wavelengths. Kerr *et al.* have used other materials that are somewhat better in this regard [10]. Ediss *et al.* [33] have investigated quartz windows, but these appear to be more lossy and difficult to match, requiring two or more plastic film matching layers. An alternative is to cut grooves with a saw or ultrasonically to create small pyramids, emulating a gradual refractive index transition [40]. Further evaluation of designs will be needed for ALMA and it seems likely that more than one type will be needed to cover all the bands.

G. Wire Grids

Wire grids make excellent polarizers [41]. Although these may be made by etching metallic films deposited on dielectric films, the best results are obtained with free-standing grids wound from BeCu or tungsten wire. Losses occur due to dissipation and leakage. For electric fields perpendicular to the grid leakage is due to displacement currents in the capacitance between the wires. This is reduced by increasing the wire spacing. For the orthogonal polarization, increasing the spacing decreases the effective shunt inductance of the grid causing more leakage for that polarization. Using formulas in [41] it is found that the leakage for the two polarizations is roughly equal for pitch to wire diameter ratios of 3–4 depending on the incidence angle of the field.

Wire diameters are commonly 10–25 μm , depending on the wavelength. Leakage losses much less than 1 % can be expected. Uniformity of wire spacing is a serious concern and experimental [42] and theoretical [43] results show that the rms spacing should be less than $\sim 10\%$ of the nominal spacing. Ohmic losses can be estimated roughly by taking the reflectivity of a solid reflector of the same material and reducing it by the wire diameter to pitch ratio.

V. OPTICAL CONFIGURATION

We consider several possible layouts for the optics. As an aid to understanding the effect of various parameters on the efficiency of the feed we use the overlap integral approach given in [44]. Radiation from a distant (point) source incident on the aperture is assumed to produce a top-hat illumination at the secondary mirror. This propagates as a beam ψ_s diffracting towards the secondary focus. Likewise, the feed horn is assumed to generate a beam ψ_f traveling out towards the secondary mirror. Standard quasi-optical theory [45] is

used to determine the propagation of these beams through free space and the optical elements. An estimate of the aperture efficiency is then given by

$$\eta = \left| \langle \psi_f | \psi_s \rangle \right|^2 \quad (6)$$

where the overlap integral may be made in any plane. When the effect of aperture stops must be estimated, the integral is most conveniently evaluated in the plane of the stop.

With this formalism we can use paraxial beam theories to propagate realistic beam patterns through the optics rather than assuming that there is only a fundamental Gaussian mode. Since the same equations describe the propagation of all modes [27] the initial design can be done with the fundamental mode and later extended to the full mode-spectrum.

Feed systems may have a simple feed horn, or a horn and several focusing and other optical components. The choice of configuration will affect the efficiency and bandwidth for coupling the telescope to the antenna.

A. Feed Horn Only

The simplest feed system is a corrugated feed horn directly illuminating the secondary mirror. This has the advantage of not requiring any optical elements with their associated dissipative and spillover losses.

To estimate the aperture efficiency, we will assume that the corrugated horn aperture is at the secondary focus and that the aperture field is a truncated zeroth order Bessel function, J_0 , [11]. We take the Airy focal spot from the antenna and calculate the overlap integral with the horn aperture field using (6). The horn aperture radius may be optimized at some frequency, but since the Airy spot scales with wavelength, there is a reduction in efficiency at other frequencies. This is illustrated in Fig. 6. Note that the maximum efficiency is 83.7 % and falls off to 75.5 % at the edges of a 40 % band. At the band center the edge taper is about 11.3 dB [44].

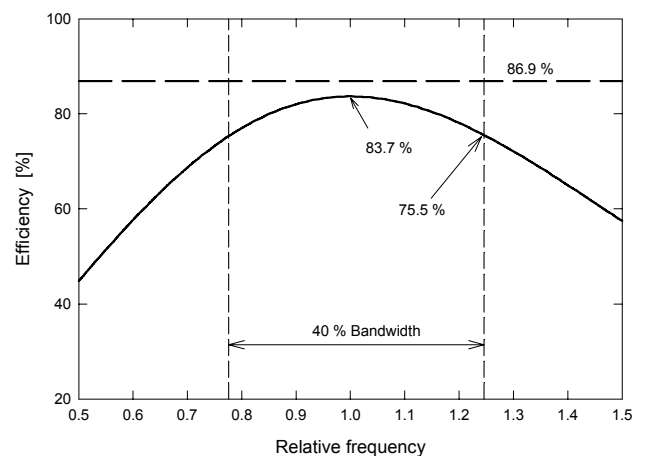


Fig. 6. Aperture efficiency for an ideal corrugated horn at the secondary focus (solid line), and at an image of the primary (dashed line).

At the focus of a Cassegrain with a primary focal ratio f/D and magnification M , the Airy spot size is $\sim \lambda M f/D$. This is

quite large for the ALMA antennas with $M=20$, so the horn will have a large aperture. The minimum length of horn can be estimated as follows.

A corrugated horn produces a beam that is very close to being Gaussian (98 % of the power is in the fundamental mode [46]). Choosing the edge taper defines the beam radius of the Gaussian beam at the secondary mirror, w_s , while the distance from the geometrical focus to the secondary sets the wavefront radius of curvature, R_s . These two values uniquely define the distance of the beam-waist from the secondary, z_s , and waist-radius, w_0 , for a give wavelength λ .

$$w_0 = \frac{w_s}{\sqrt{1 + \left(\frac{\pi w_s^2}{\lambda R_s}\right)^2}} \quad (7)$$

$$z_s = \frac{R_s}{1 + \left(\frac{\lambda R_s}{\pi w_s^2}\right)^2} \quad (8)$$

Usually the horn is assumed to be long enough to have a negligible wavefront curvature at its aperture putting the waist close to the horn aperture, but this requires a very long horn. In general the horn can be located anywhere along the Gaussian beam as long as the aperture radius is $w/0.6436$, and its length is R , where w and R are the beam radius and wavefront radius of curvature of the beam in the plane of the horn aperture (Fig. 7). The shortest horn will therefore have its aperture at the confocal point of the beam where the wavefront radius of curvature is smallest. This is a distance [45]

$$z_c = \frac{\pi w_0^2}{\lambda} \quad (9)$$

from the waist. In this plane the beam radius is

$$w = \sqrt{2} w_0 \quad (10)$$

and the wavefront radius of curvature is

$$R = 2z_c \quad (11)$$

Such a horn is known as an optimum gain horn* [22].

Assuming that the secondary mirror is in the far-field of the waist, the waist radius required to give an edge taper of T_E in dB is

$$w_0 = \frac{2\lambda Mf/D}{\pi} \sqrt{\frac{T_E[\text{dB}]}{20} \ln(10)} \quad (12)$$

For the ALMA receivers the secondary focal ratio is $Mf/D=8$ [47]. At the center frequency for Band 2 of 78.5 GHz with an 11 dB edge taper we get $w_0 = 21.9$ mm and $z_c = 394$ mm, for example. To launch this the corrugated horn

would have an aperture diameter of 96 mm and a length of 790 mm. Clearly this is impractical and we have to use some re-focusing element(s).

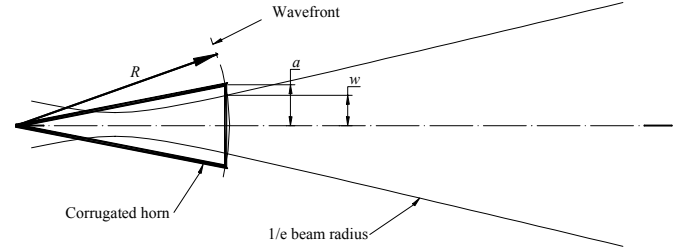


Fig. 7. Relationship between a corrugated horn and the associated best-fit fundamental Gaussian beam mode.

Coupling efficiency with an optimum gain horn will also have some frequency dependence, but less than a zero aperture phase error horn located at the secondary focus.

Profiling has been used to reduce the lengths of corrugated horn [11]. I have not investigated this but suspect that it will not work very well for horns with an aperture diameter large compared to a wavelength. This is because the walls of the horn influence mainly the field close to them. The wavefront would be modified there but not at the center of the horn, resulting in a distortion of the wavefront. The large electrical size may make it difficult to verify this using mode-matching techniques. In any case the reduction in length would not be sufficient for practical purposes, the aperture radius would still be large, and the efficiency frequency-dependent.

We must therefore consider a system with at least a lens or refocusing mirror.

B. Corrugated Horn and Lens

There are two ways of using a lens with a feed horn. One is the “lens-corrected horn” where the lens is at the aperture of the horn to make the aperture wavefront planar. Although this removes the restriction on horn length it does not reduce the aperture diameter or the frequency dependence.

The other arrangement is to have the lens further from the horn aperture and to refocus the beam (Fig. 8). A common scheme is to have a relatively small feed with a nearly uniform aperture field phase located at one focus of the lens. The other focal point is at the secondary focus of the telescope. This can be viewed as re-imaging the secondary mirror on to the feed aperture. Efficiency can then be calculated by taking the overlap of the feed field at the secondary mirror and a top-hat function (Eq. 6), which yields an efficiency of 86.9%, independent of frequency for the correct choice of beam size. This is plotted in Fig. 6, which shows that this configuration has a higher efficiency than the simple horn alone, even at its design center frequency. This is the standard against which any optical system should be compared.

* Incidentally, insects discovered optimum gain horns and corrugated feeds several million years ago.

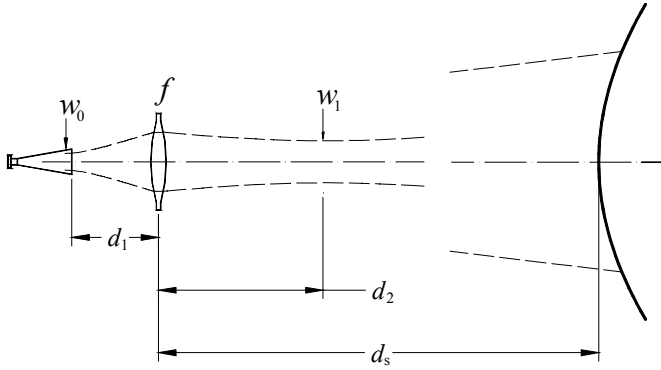


Fig. 8. A corrugated horn and lens used to illuminate the secondary mirror. The lens allows a smaller horn to be used, and to have frequency independent illumination.

The actual edge taper for this case is 10.0 dB, while the edge taper for the corresponding best-fit Gaussian is 12.3 dB. The image of the horn has a diameter of 1.306 times the secondary mirror diameter.

C. Frequency Independent Design

In Section B it was assumed that the illumination was frequency independent. However, this is not precisely true if the beam-waist is at the secondary focus except in the limit of zero wavelength. In general the waist will be located farther from the secondary mirror to give the correct radius of curvature. The optics can be designed to give the appropriate waist position as a function of frequency, however.

There are several equivalent ways of stating the appropriate conditions. Clearly, frequency-independence includes infinite frequency, or Geometrical Optics, so that ray tracing results apply and standard optics imaging equations may be used. Probably the first to expressly show that diffractive optics could be essentially frequency independent was Chu [48] who used the Fresnel integral and derived the same equations as for Gaussian Optics (*i.e.*, paraxial ray optics). In an *ABCD*-matrix formulation [45], the *B* element must be zero. Finally, the total phase slippage, ϕ , for a Gaussian beam [49] accumulated between the horn aperture and the secondary mirror should be equal to π [50].

By applying any one of these criteria a broad-band illumination system may be designed with several lenses or mirrors. To approach this ideal it is also necessary that beam truncation is minimized and that the focusing elements can be well approximated by pure phase transformers. Some guidelines for the required beam clearances are given in the following Section.

D. Beam Truncation Criteria

An alternative calculation of the aperture efficiency is obtained by evaluating the overlap integral at the secondary focus. This yields an identical answer to that in the previous section if the integral is taken over an infinite plane. By taking the integral over a finite radius the effect of aperture stops (such as dewar windows) can be estimated. The integral

is over the product of the far-field pattern of the horn (produced by the lens) and the Airy pattern. Fig. 9 compares the two fields. Evidently, the higher efficiency in this case results from the partial interception of energy in the first Airy ring.

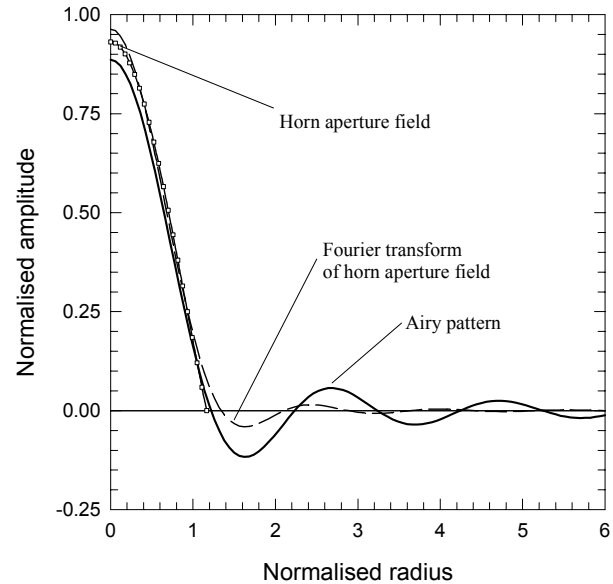


Fig. 9. Aperture field and imaged field (Fourier transform) from a corrugated horn compared with the Airy pattern at the secondary focus of the antenna.

Fig. 10 shows the reduction in efficiency as a function of stop radius*. Virtually all the efficiency is obtained when the first Airy ring is enclosed,

$$r = 2.33\lambda Mf / D \quad (13)$$

and only 1% is lost if

$$r = 1.86\lambda Mf / D \quad (14)$$

In terms of the best-fit Gaussian beam these correspond to an aperture diameter of $5.9w$ and $4.9w$ respectively. If, as is often the case, the lens is close to the secondary focus this will also be a good measure of the required size of the lens. Table II gives the minimum aperture sizes at the secondary focus to avoid losses greater than 1%.

We note that the amount of clearance required in the beam depends on the location of the stop relative to the horn or the secondary mirror. A truncation diameter of only $3.11w$ at the horn aperture (or an image of it) will pass the *entire* beam. In general, close to the horn aperture or an image of it smaller stops can be tolerated, but in the far-field a greater clearance must be allowed. The transition between the two regimes is at $\sim z_c$. This factor of almost two in acceptable stop size is a result of the higher-order modes which account for only 2% of the feed pattern energy. Murphy *et al.* [51] present a detailed

* It is often assumed that a loss of 1% from a beam is a loss of 1% in efficiency. In fact it can be seen from Eq. (6) that the efficiency is reduced by 2% since there is a product of amplitudes squared.

study of truncation for beams radiated by various types of horn.

TABLE II.

MINIMUM APERTURE DIAMETERS FOR A WINDOW AT THE CASSEGRAIN FOCUS THAT WILL DEGRADE APERTURE EFFICIENCY BY LESS THAN 1 %.

Band	Lowest frequency [GHz]	Highest frequency [GHz]	5 w Window diameter [mm]
1	31.5	45	351
2	67	90	165
3	89	116	124
4	125	163	88
5	163	211	68
6	211	275	52
7	275	370	40
8	385	500	29
9	602	720	18
10	787	950	14

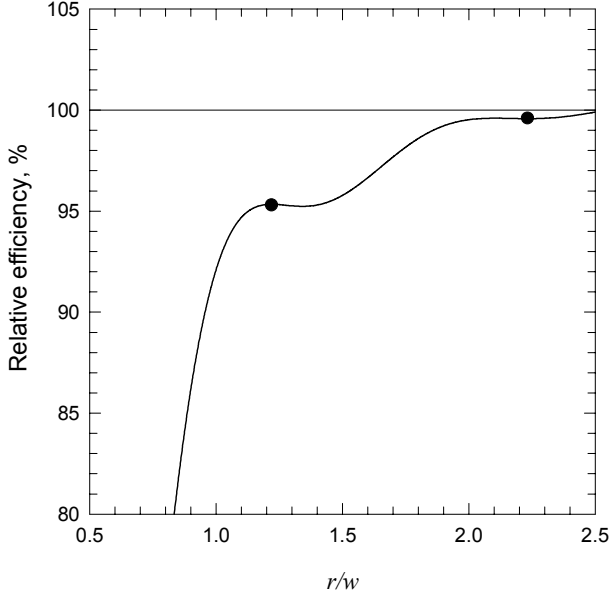


Fig. 10. Effect of a circular aperture of radius r at the secondary focus on the antenna aperture efficiency. w is the radius of the Gaussian fundamental mode which is a best fit to a corrugated horn field.

E. Optical System With Optimum Gain Horn

To get a feeling for the parameter values for a simple optical system we will analyze an optimum gain horn with a lens. To simplify the problem we assume that the horn/lens combination produces a waist at the secondary focus. While this is true only at short wavelengths the values will change only slightly when the correct focusing conditions are imposed. Under these assumptions the problem may be parameterized by a single quantity which we choose to be the

beam radius at the horn aperture $w_a = 0.6436$ (Fig. 7 and Fig. 8).

The lens is assumed to be a pure phase transformer so that the beam sizes on the left and right sides must be identical allowing d_2 to be written in terms of d_1 . The phase from the horn aperture to the secondary mirror is approximately

$$\phi = \arctan\left(\frac{d_1 + \Delta}{z_{c1}}\right) - \arctan\left(\frac{\Delta}{z_{c1}}\right) + \arctan\left(\frac{d_2}{z_{c2}}\right) + \frac{\pi}{2} \quad (15)$$

which is set equal to π for frequency independence.

By applying these criteria we find the following (β is a parameter relating the beam width to the secondary mirror size and $\beta = 2.379$ for optimum efficiency):

Length of the horn:

$$\frac{L_h}{\lambda} = \pi \left(\frac{w_a}{\lambda}\right)^2 \quad (16)$$

Distance from horn aperture to lens:

$$\frac{d_1}{\lambda} = \beta \frac{f/D}{w_a/\lambda} \quad (17)$$

Distance of lens from secondary focus:

$$\frac{d_2}{\lambda} = \left(\frac{\pi w_a}{\lambda} + \beta f/D\right) \frac{\beta f/D}{\pi} \quad (18)$$

The lens focal length is found from the inverse of the sum of the beam wavefront curvatures on the two sides of the lens:

$$\frac{f_L}{\lambda} = \beta f/D \frac{w_a}{\lambda} \quad (19)$$

For a $5w_L$ diameter lens the focal ratio is:

$$\frac{f}{5w_L} = \frac{\pi w_a}{5} \left(\left(\frac{w_a \pi}{\beta f/D} + 1 \right)^2 + 1 \right)^{-1/2} \quad (20)$$

For an offset mirror the amplitude distortion and cross-polarization are controlled by the ratio of the beam size to the mirror focal length, which is

$$\frac{w_L}{f} = \frac{l}{\pi w_a} \left(\left(\frac{w_a \pi}{\beta f/D} + 1 \right)^2 + 1 \right)^{1/2} \quad (21)$$

Some these quantities are shown in Fig. 11 in a wavelength independent form. Horn apertures of at least 4λ are required to have a lens or mirror with an f-ratio greater than 1. This means that the horn flare angle will be less than about 10° .

F. Horn and Multiple Lenses or Mirrors

The same imaging principles apply to systems with multiple focusing elements. A horn/lens combination may be used to make an image of the horn aperture relatively close to the

lens (rather than at the secondary mirror) and a second lens used to re-image that on to the secondary. This can obviously be repeated with an arbitrary number of focusing elements. Geometrical imaging may therefore be used for frequency independent design as before, and Gaussian beams used to find suitable clearances. Again, clearances need to be $>5w$ near the secondary focus or images of it, but can be smaller near images of the feed aperture.

The addition of extra focusing elements adds some flexibility that may offset the extra losses. For example, cross-polarization cancellation is feasible with suitably chosen conic-section reflectors (Sec. IV.D), or intermediate waists (foci) can be produced to minimize window sizes and associated IR loading.

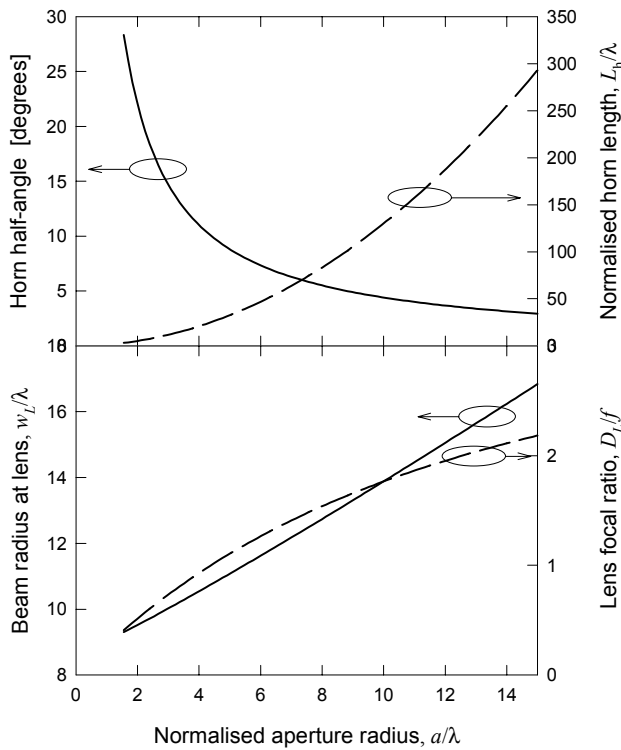


Fig. 11. Some of the optical parameters for a system with an optimum gain horn and a single focusing element, calculated for an antenna with a secondary focal ratio of $f/8$.

VI. EXAMPLE DESIGN

As an example of the application of the above design ideas we consider ALMA Band 3 (84–116 GHz). At the lowest frequency the $5w$ diameter of the beam at the secondary focus is about 125 mm. A window into the dewar with this clearance would present a huge IR thermal load, so the beam must be focused down by a factor of $\sim 3-5$ (9–25 in area). This can be achieved with an ellipsoidal mirror. In this band the polarizations may be separated in waveguide so no space allowance needs to be made for an optical diplexer.

If the window diameter is to be about 30 mm the feed aperture should be somewhat smaller, say 25 mm. To get the distance from the feed to the ellipsoid, we multiply the dis-

tance to the secondary (6 m) by the ratio of the feed aperture to the desired image size of the feed (1.306 times the secondary mirror size), giving 153 mm. At 84 GHz the optimum gain horn with an aperture of 25 mm is about 57 mm long and has a flare angle of 12.4° . The precise calculation of the optical parameters shows that the ellipsoid has a focal length $f = 164.5$ and is at a distance $d = 168.7$ mm from the horn aperture. An ellipsoid with a diameter of $5w$ has an f -ratio of about 0.83. There will be an associated co-polar distortion loss of about 0.25 % and a cross-polar power of 0.5 %, for a 30° incidence angle.

A disadvantage of this choice of parameters is that the beam divergence is large enough to make the window size significantly larger than the horn aperture. Using a longer horn will reduce the beam divergence and shift the waist towards the horn aperture. Since the space between the horn and mirror is more critical than the length of the horn it is acceptable to extend the horn to 140 mm. The optical parameters are now $f = 157.6$ mm, $d = 161.6$ mm, and the mirror has an f -ratio of 1.1. The smaller mirror and reduced beam divergence permit a smaller angle of incidence also reducing distortion and cross-polar content to $\sim 0.15\%$ and $\sim 0.3\%$. Fig. 12 illustrates the geometry, with a plane mirror added to direct the beam up towards the secondary. The mirrors are large enough to capture the $5w$ beam diameter. The hole in the shield can be smaller than this since it is close to the feed aperture. The window is made from HDPE and is two wavelengths thick, with quarter-wave matching grooves machined on both sides. Below that is an expanded polystyrene foam infrared filter.

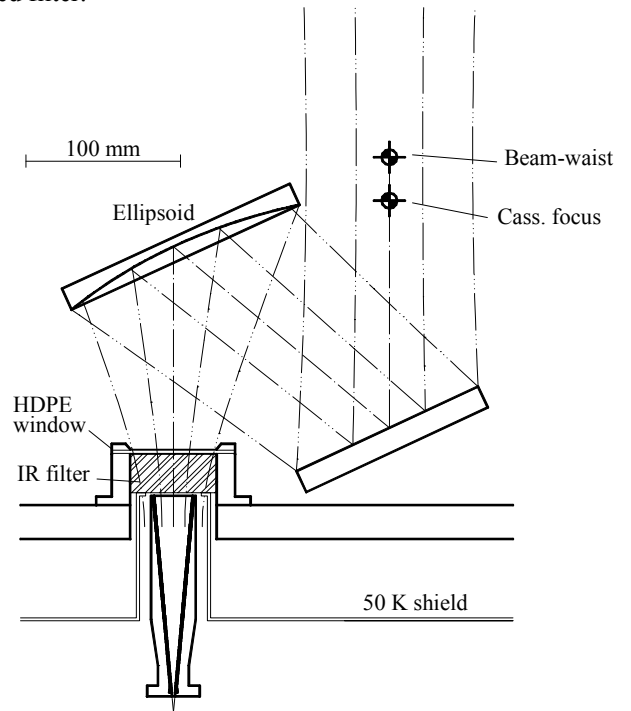


Fig. 12. Possible optical design for Band 3. The beam contours denote the w and $2.5w$ radii of the nominal Gaussian beam. See text for details of windows, filter, etc.

Although a full computation of the radiation pattern is complicated, a simple numerical integration assuming circular symmetry can give a good idea of the effectiveness of the design [50]. Calculations for two frequencies, taking into account the window and mirror stops is shown in

Fig 13. The pattern is very close to being an image of the horn aperture field, which is also shown in the diagram. There is negligible phase error, so that no refocusing of the secondary as a function of frequency is required.

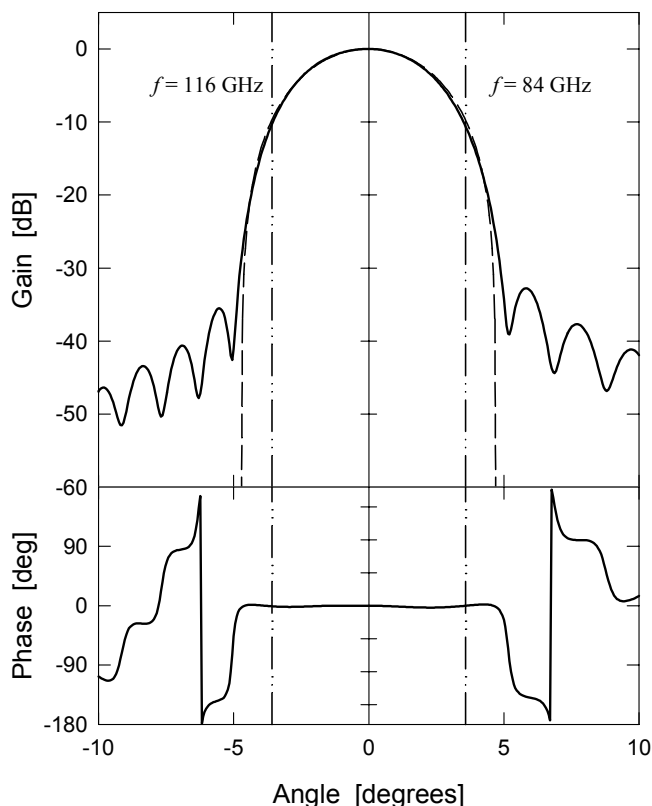


Fig 13. Beam patterns calculated for the design given in the text. The dashed line shows the function $J_0(r)$, the ideal corrugated horn aperture field. Dash-dot-dot line indicate the edges of the secondary mirror. The phase is relative to a sphere centered on the geometrical secondary focus.

Estimates of the various losses in the optics are shown in Fig. 14. The total loss is estimated to be less than $\sim 3.5\%$ across the band. One of the main contributions is the truncation loss due to the various apertures. Some of this will be reflected back to the dewar, part to ambient, and some on to the sky. It probably accounts for an additional 1–2 K in noise. A significant contribution comes from the foam used for the IR filter. Since the foam supports a temperature gradient from the upper face to the lower the average physical temperature will be less than the ambient temperature. Its noise contribution will therefore be ~ 1 K or less. The window is at ambient temperature and will contribute of order ~ 0.8 K to the noise, and the mirrors together add about 1.4 K due to ohmic losses. The Ruze scattering due to small scale errors in the mirror surfaces will be terminated at ambient, but this will be less than ~ 0.1 K.

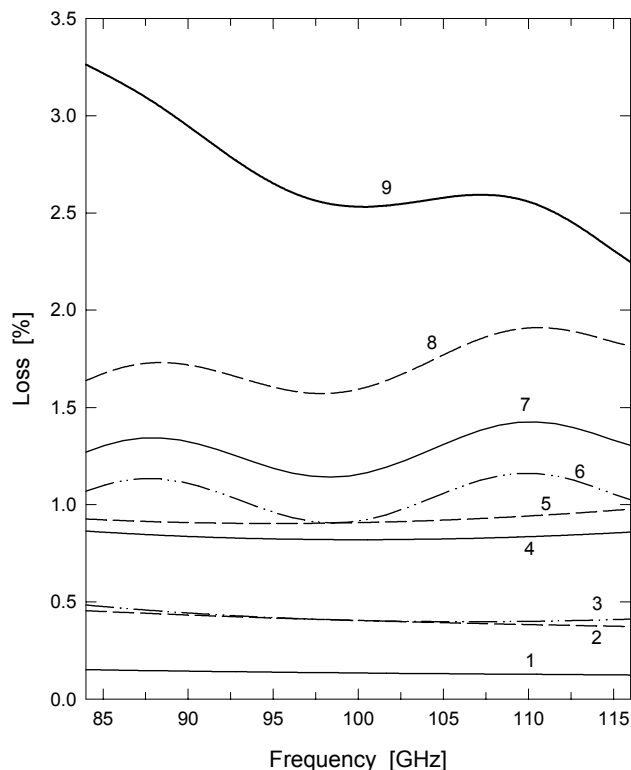


Fig. 14. Estimated optical losses for the example Band 3 design. The curves give the cumulative loss for (1) amplitude distortion, (2) cross-polar, (3) aberrations, (4) ohmic losses, (5) surface error (Ruze), (6) window reflection, (7) window dissipation, (8) IR filter loss, (9) truncation losses.

VII. GENERAL DISCUSSION AND CONCLUSIONS

From the perspectives of sensitivity, manufacturing, and reliability the simplest system possible is desirable. Optical systems for ALMA should, if possible, comprise only a few lenses or ellipsoidal mirrors and, for the higher frequency bands, wire grid polarizers and dielectric beam-splitters for LO injection. Some of the functions which have been done in the optics in previous systems such as image rejection and conversion of polarization states may be done by post-processing.

Complexity in the optics may be justified only if it will enhance sensitivity. Sideband rejection could achieve this if the degradation due to the added optics is less than the improvement in rejecting sky noise. This issue is complicated since it involves the receiver noise temperature, IF frequency and bandwidth, diplexer Ohmic and overlap losses, observing modes and atmospheric conditions [52], [53], [54], [55]. However, it is clear that the additional elements add significant complexity and bring reliability and maintenance issues which must also be considered in the decision.

An important factor in the final optical design will be the influence of the cryostat on the layout. This poses a significant space limitation that will be felt particularly in the lower frequency bands. Most of the compromises will have to be

made there, while the high frequencies will be relatively unrestricted.

As shown in the example design it is necessary to have some external optics for the low-frequency designs. Thus the optics have to allow for vacuum windows and IR filters between optical elements. On the other hand, some of the high-frequency band optics may be contained entirely within the dewar since the windows are already small without external refocusing of the beam. This gives more freedom in the choice of optical design parameters.

In the end, the design has to be a compromise among several conflicting requirements. Some elements are not required at all for the optical design but have to be in the optical path, namely the vacuum windows and infrared filters. More detailed studies will be required to best satisfy the need for strength, infrared blocking, vapor permeability and so forth.

Because of the excellent site and antennas all efforts have to be made to minimize optical losses. A key factor will be to verify that all materials are tested at the frequencies at which they will be applied. Setups for verification of dielectric constant, absorption coefficient, reflectivity, uniformity, etc. will be essential. Components should also be rigorously tested.

While the general principles of optics for ALMA are generally clear, there remain several areas for further study. The principal of these are optimization of designs for windows and IR filters. In addition the challenges of production of significant quantities of components has to be faced.

REFERENCES

- [1] A. R. Thompson, J. M. Moran, and G. W. Swenson Jr, *Interferometry and Synthesis in Radio Astronomy*. Malabar: Krieger, 1998.
- [2] J. W. Lamb, "Miscellaneous data on materials for millimeter and submillimeter optics", *Int. J. IR and Millimeter Waves*, vol. 17, no. 12, pp. 1997-2034, Dec. 1996.
- [3] F. J. Fischer, "Excess conduction losses at millimeter wavelengths," *IEEE Trans. Microwave Theory Tech.*, vol. MTT-24, no. 11, pp. 853-858, Nov. 1976.
- [4] M. Born and E. Wolf, *Principles of Optics*, Oxford: Pergamon Press, 1980.
- [5] J. D. Cook, J. W. Zwart, K. J. Long, V. O. Heinen, and N. Stankiewicz, "An experimental apparatus for measuring surface resistance in the submillimeter-wavelength region," *Rev. Sci. Instrum.*, vol. 62, no. 10, pp. 2480-2485, Oct. 1991.
- [6] H. Matuso, J. Inatani, N. Kuno, K. Miyazawa, K. Okumura, T. Kasuga, and H. Murakami, "Submillimeter-wave telescope onboard a sounding rocket," *SPIE Proc.*, San Diego, 1994.
- [7] A. J. Gatesman, R. H. Giles, and J. Waldman, "High-precision reflectometer for sub-millimeter wavelengths," *J. Opt. Soc. Am. B*, vol. 12, no. 2, pp. 212-219, Feb. 1995.
- [8] J. J. Bock, M. K. Parikh, M. L. Fischer, and A. E. Lang, "Emissivity measurements of reflective surfaces at near-millimeter wavelengths," *Appl. Optics.*, vol. 34, no. 22, pp. 4812-4816, Aug. 1995.
- [9] A. F. Clarke, G. E. Childs, and G. H. Wallace, "Electrical resistivity of some engineering alloys at low temperatures," *Cryogenics*, vol. 10, pp. 295-305, August 1970.
- [10] A. R. Kerr, N. J. Bailey, D. E. Boyd and N. Horner, "A study of materials for a broadband millimeter-wave quasi-optical vacuum window," NRAO, Millimeter Array Memo Series No. 90, Aug. 1992
- [11] P. J. B. Clarricoats and A. D. Olver, *Corrugated Horns for Microwave Antennas*. London: Peter Peregrinus, 1984.
- [12] B. N. Ellison, M. L. Oldfield, D. N. Matheson, B. J. Maddison, C. M. Mann, and A. F. Smith, "Corrugated feedhorns at terahertz frequencies - preliminary results," in *5th International Symposium on Space Terahertz Technology*, Ann Arbor, USA, 1994.
- [13] A. W. Love, "The diagonal horn antenna," *Microwave Journal*, vol. 5, pp. 117-122, Mar. 1962.
- [14] P. D. Potter, "A new horn antenna with suppressed sidelobes and equal beamwidths," *Microwave Journal*, vol. 6, pp. 71-78, 1963.
- [15] X. Zhang, "Design of conical corrugated feed horns for wide-band high-frequency applications," *IEEE Trans. Microwave Theory Tech.*, vol. 41, no. 8, pp. 1263-1274, Aug. 1993.
- [16] J. W. Lamb, "ALMA evaluation receiver optics design," ALMA Internal Report, April 2000.
- [17] A. Wootten, L. Snyder, E. van Dishoeck, and F. Owen, "Frequency band considerations and recommendations," NRAO, ALMA Millimeter Array Memo Series No. 213, May 2000.
- [18] D. Hoppe, "CWGSCAT" a program package developed at JPL, distributed by COSMIC Co.
- [19] J. Zmuidzinas and H. G. LeDuc, "Quasi-optical slot antenna SIS mixers," *IEEE Trans. Microwave Theory Tech.*, vol. 40, pp. 1797-1804, Sep. 1992.
- [20] J. W. Lamb, "Cross-polarization and astigmatism in matching grooves", *Int. J. IR and Millimeter Waves*, vol. 17, no. 12, pp. 2159-2165, Dec. 1996.
- [21] P.-S. Kildal, "Meniscus-lens-corrected corrugated horn: a compact feed for a Cassegrain antenna," *IEE Proc. Part H*, vol. 131, no. 6, pp. 390-394, Dec. 1984.
- [22] R. Padman, J. A. Murphy, and R. E. Hills, "Gaussian mode analysis of Cassegrain antenna efficiency," *IEEE Trans. Antennas and Propagat.*, vol. AP-35, pp. 1093-1103, 1987.
- [23] J. A. Hudson, R. Plambeck, and W. J. Welch, "Aperture efficiency enhancement in a Cassegrain system by means of a dielectric lens," *Radio Science*, vol. 22, pp. 1091-1101, Nov. 1987.
- [24] J. W. Lamb, "Illumination shaping with a lens," *Proc. European Workshop on Low-Noise Quasi-Optics*, Bonn Sept. 1994.
- [25] J. A. Murphy, "Distortion of a simple Gaussian beam on reflection from off-axis ellipsoid mirrors," *Int. J. Infrared and Millimeter Waves*, vol. 8, no. 9, pp. 1165-87, 1988.
- [26] C. Dragone, "Off-set multireflector antennas with perfect pattern symmetry and polarization discrimination," *Bell System Tech. J.*, vol. 57, pp. 2663-2684, 1978.
- [27] D. H. Martin and J. W. Bowen, "Long-wave optics," *IEEE Trans. Microwave Theory Tech.*, vol. 41, no. 10, pp. 1676-1689, Oct. 1993.
- [28] T.-S. Chu, "Polarization properties of offset dual-reflector antennas," *IEEE Trans. Antennas and Propagat.*, vol. 39, no. 12, pp. 1753-1756, Dec. 1991.
- [29] S. Withington, J. A. Murphy, A. Egan, and R. E. Hills, "On the design of broadband quasi-optical systems for submillimeter-wave radio-astronomy receivers," *Int. J. Infrared and Millimeter Waves*, vol. 13, no. 10, pp. 1515-1537, Oct. 1992.
- [30] J. Ibruegger, "Transmission of room-temperature radiation by materials at low temperatures," *Int. J. IR and Millimeterwaves*, vol. 5, no. 5, May 1984.
- [31] J. W. Lamb, "Infrared filters for cryogenic millimeterwave receivers," *Int. J. Infrared and Millimeter Waves*, vol. 14, no. 5, pp. 959-967, 1993.
- [32] R. Padman, "Reflection and cross-polarisation properties of grooved dielectric panels," *IEEE Trans. Antennas Propagat.*, vol. AP-26, no. 5, pp. 741-743, Sep. 1978.
- [33] G.A. Ediss, A.R. Kerr, and D. Koller, "Measurements of quasi-optical windows with the HP 8510," NRAO, ALMA Memo Series No. 295, Mar. 2000.
- [34] G. E. Childs, L. J. Ericks, and R. L. Powell: *Thermal Conductivity of Solids at Room Temperature and Below*, NBS Monograph 131, 1973.
- [35] Norton Performance Plastics, Wayne, New Jersey, (204) 696-4700
- [36] D. J. Benford, M. C. Gaidis, and J. W. Kooi, "Transmission properties of Zitex in the infrared to the submillimeter," in *Proc. Of the 10th Int. Symp. On Space THz Tech.* (T. Crowe, ed.), pp. 405-413, 1999.
- [37] J. S. Clarke L. R. D'Addario, "Tests of materials for use in multi-layer infrared filters in cryogenic application," NRAO, ALMA Memo Series No. 269, Aug. 1999.
- [38] J. Zmuidzinas, private communication.

- [39] W. Grammer, "Analysis of reflective gratings as infrared filters," NRAO, ALMA Memo Series Memo No. 275, Sep. 1999.
- [40] J. Y. L. Ma and L. C. Robinson, "Night moth eye window for the millimeter and sub-millimeter wave region," *Optica Acta*, vol.30, no. 12, pp. 1685–1695, 1983.
- [41] T. Larsen, "A survey of the theory of wire grids," *IRE Trans. Microwave Theor. Tech.*, vol. MTT-10, pp. 191–201, May 1962.
- [42] J. B. Shapiro and E. E. Bloemhof, "Fabrication of wire-grid polarizers and dependence of submillimeter-wave optical performance on pitch uniformity," *Int. J. Infrared and Millimeter Waves*, vol. 11, no. 8, pp. 973–980, 1990.
- [43] M. Houde, R. L. Akeson, J. E. Carlstrom, D. A. Schleunig, J. W. Lamb and D. P. Woody, "Polarizing grids, their assemblies and beams of radiation," in press, *PASP*, May 2001.
- [44] J. W. Lamb, "Quasioptical coupling of Gaussian beam systems to large Cassegrain antennas," *Int. J. Infrared and Millimeter Waves*, vol. 7, no 10, pp. 1511-1536, 1986.
- [45] P. F. Goldsmith, "Quasi-optical techniques at millimeter and submillimeter wavelengths," in *Infrared and Millimeter Waves, Vol 6*, K. J. Button, Ed., New York: Academic Press, 1982.
- [46] R. J. Wylde, "Millimetre wave Gaussian beam-mode optics and corrugated feed horns," *Proc. IEE*, Pt H, 1984, vol. 13, pp. 258–262
- [47] J. W. Lamb, "Optimized optical layout for MMA 12-m antennas," NRAO, Millimeter Array Memo Series No. 246, January 1999.
- [48] T.-S. Chu, "An imaging beam waveguide feed," *IEEE Trans Antennas and Propagat.*, vol. AP-31, no. 4, pp. 614–619, July 1983.
- [49] P. F. Goldsmith, "Quasi-optical techniques at millimeter and submillimeter wavelengths," in *Infrared and Millimeter Waves, Vol. 6*, K. J. Button, Ed., New York: Academic Press, 1982.
- [50] J. W. Lamb, "Quasioptical systems for antennas," in *Proc. 20th ESTEC Antenna Workshop on Millimetre Wave Antenna Technology and Antenna Measurements*, pp. 15-24, Noordwijk, 18-20th June 1997.
- [51] J. A. Murphy, A. Egan, and S Withington, "Truncation in Millimeter and submillimeter-wave optical systems," *IEEE Trans. Antennas. Propagat.*, vol. 41, no. 10, pp. 1408–1413, October 1993.
- [52] A. R. Thompson and A. R. Kerr, "Relative sensitivities of single and double sideband receivers for the MMA," NRAO, MMA memo Series No. 168, Apr. 1997.
- [53] P. R. Jewell and J. G. Mangum, "System temperatures, single versus double sideband operation, and optimum receiver performance," NRAO, MMA Memo Series No. 170, May 1997.
- [54] J. W. Lamb, "SSB vs. DSB for submillimeter receivers," NRAO, ALMA Memo Series No 301, Apr. 2000.
- [55] A. R. Thompson and L. D'Addario, "Relative sensitivity of double- and single-sideband systems for both total power and interferometry," NRAO, ALMA Memo Series No. 304, Apr. 2000.